Pré-Publicações do Departamento de Matemática
Universidade de Coimbra
Preprint Number 10–13

FLUX TRACKING IN DELIVERY POLYMERIC SYSTEMS

J.A. FERREIRA, P. DE OLIVEIRA, P. M. DA SILVA AND L. SIMON

Abstract: The dynamics of diffusive and stress-induced transport in polymeric delivery systems was investigated. Partial and ordinary differential equations were first written to describe drug release behaviors in Maxwell and Maxwell-Voigt materials. The time constants governing the flux and concentration responses of a permeating species were determined from a Laplace transform solution of the original model. A "tracking strategy", based on the estimated characteristic times, was proposed to estimate the delivery rate and the concentration near the exit side of the membrane. The methodology was more efficient at times greater than the time constant and the prediction error decreased further as the process approached steady state. Numerical illustrations and comparisons made with published data show the effectiveness of the proposed approach in describing the influence of the Young modulus, viscosity and relaxation time on the transient regime.

Keywords: Controlled drug delivery, visco-elasticity, effective time, mathematical model, Laplace Transforms.

1. Introduction

A central problem in release technology is to combine a diffusing species with a polymeric matrix to obtain a delivery profile suitable for a particular situation or treatment. Apart from controlled drug delivery, other applications include removal of solvent from polymer solutions during dry spinning, diffusional release of pollutants and additives from polymers into the environment and controlled release of agriculture chemicals. Relationships between polymer matrix systems and drug release have been studied these past few years by several researchers. Some of these studies have been experimental in nature and aimed at establishing empirical relations between the amount of drug released and pertinent mechanical polymer properties, such as the viscosity and Young modulus ([2],[3],[18]). Other groups include a mathematical description of the process in their investigations to simulate the flux ([9],[10]). An essential step toward an in-depth understanding of delivery

Received May 17, 2010.
This work was partially supported by Projects:PTDC/MAT/74548/2006, UTAustin/MAT/0066/2008.

phenomena is an examination of the relationship between the flux, concentration or response time on the characteristic properties of the polymeric system. Our aim, in this paper, is to conduct such a study and develop a "tracking strategy", that consists of a set of *a priori* estimations of the concentration and/or flux and the times it takes to reach these values. Analytical equations for the steady fluxes and the response times are established in terms of parameters that characterize the polymer and the permeant. To describe the behavior of the polymeric membrane, we consider a class of viscoelastic models, where diffusive and mechanical properties are coupled. The selection of these models is motivated by the descriptions proposed in [9], [4] and [7] and is represented by the system of partial and ordinary differential equations

$$u_t = Du_{xx} + D_v\sigma_{xx}\,,\ x \in (0,h)\,, t > 0, \tag{1}$$

$$\sigma_t + \beta\sigma = \alpha\varepsilon + \gamma\varepsilon_t\,,\ x \in (0,h),\ t > 0. \tag{2}$$

In (1)-(2), u stands for the concentration of the diffusing species, σ stands for the stress, ε for the strain, D represents the diffusion coefficient, h the thickness of a membrane and D_v, α, β, γ are related with properties of the polymer. Their meaning will become clear in Section 2. Even if equation (2) does not represent the most general form of a linear relation between strain and stress, it accounts for a wide range of visco-elastic behaviors. A more realistic description of some processes would require the use of a non linear relation between strain and stress. However, in the case of drug delivery, polymeric devices undergo small strains, so the physics of the problem can be modeled by linear equations where parameters are determined in order to fit experimental results. As described in Section 2, different linear visco-elastic models can be obtained as a particular case of (2). We mention, for example, two parameter models as Maxwell model and three parameters models as Maxwell-Voigt model ([4],[1]). Generalized Maxwell model is not described by constitutive equations of type (2). However, the procedures followed in this contribution can be readily adapted to that case. In (1)-(2) there are three unknowns. To eliminate the strain, it will be considered proportional to the species concentration u. We note that in (1)-(2), D, D_v, α, β and γ can depend on u. Nevertheless, these parameters will be treated as constants, in this work, to allow analytical manipulations within the framework of Laplace Transforms. In addition, when working in a regime where the

polymer is either in the rubbery or the glassy state, β and D are nearly invariant within states. As far as D is concerned, Siegel and Langer [11] show that the delay in drug release from polymers is due more to pore constrictions than a concentration-dependent diffusion. Appropriate initial and boundary conditions are given to complete the model:

$$\begin{cases} u(0,t) = u_0 \\ u(h,t) = 0 \end{cases}, \tag{3}$$

$$u(x,0) = \sigma(x,0) = 0. \tag{4}$$

The equations in (3) mean that a source of concentration u_0 is placed at the extremity $x = 0$; a perfect sink condition is assumed at $x = h$. An alternative and more realistic condition at this extremity is

$$J(h,t) = -\mu u(h,t), \tag{5}$$

where J is the flux and μ a transference coefficient. If (5) is considered, the methods developed in the present work lead to analogous results but involve tedious computations. For the sake of clarity, only the sink condition is considered here. Appendix I presents the results obtained with condition (5).

Two characteristics of the delivery process should be known when defining a "tracking strategy": the fluxes (or concentrations) of the permeating species and the times when these values are reached. Such a strategy is designed, using the concept of an effective time constant [6], to estimate *a priori* concentrations and fluxes of an agent through a membrane. The effective time is defined as

$$t_{eff}(x) = \frac{\int_0^\infty t(g^s(x) - g(x,t))dt}{\int_0^\infty (g^s(x) - g(x,t))dt}, \tag{6}$$

where $g(x,t)$ stands for a system state variable and $g^s(x)$ is the steady state of $g(x,t)$: $g^s(x) = \lim_{t \longrightarrow \infty} g(x,t)$. The effective time can be viewed as the first moment associated with the probability density function

$$d(x,t) = \frac{g^s(x) - g(x,t)}{\int_0^\infty (g^s(x) - g(x,t))dt}, \tag{7}$$

and consequently, for every x, it represents the mean time to reach an equilibrium state.

It is possible to compute t_{eff} without explicit knowledge of the analytical form of the concentration, or the flux, because

$$t_{eff}(x) = \lim_{p \longrightarrow 0} \frac{\frac{g^s(x)}{p^2} - \frac{\partial \overline{g}}{\partial p}(x,p)}{\frac{g^s(x)}{p} - \overline{g}(x,p)}, \tag{8}$$

as explained in [6]. The function $\overline{g}$ represents the Laplace transform of g. The effective-time-constant approach has been used recently by Simon in [13] for enhanced diffusion problems; the model predictions showed very good agreement with experimental results. A typical density function, for $x = h$, is represented in figure 1. A qualitative analysis of the properties of (1)-(2) and an inspection of different examples of density functions $d(x,t)$ reveal its exponential-like character, away from $t = 0$, which suggests that, for every x, $d(x,t)$ can be approximated by an exponential probability density function

$$d^*(x,t) = \frac{1}{t_{eff}} e^{-t/t_{eff}}. \tag{9}$$

We note that (7) and (9) are equivalent to approximating the flux $g(x,t)$ by

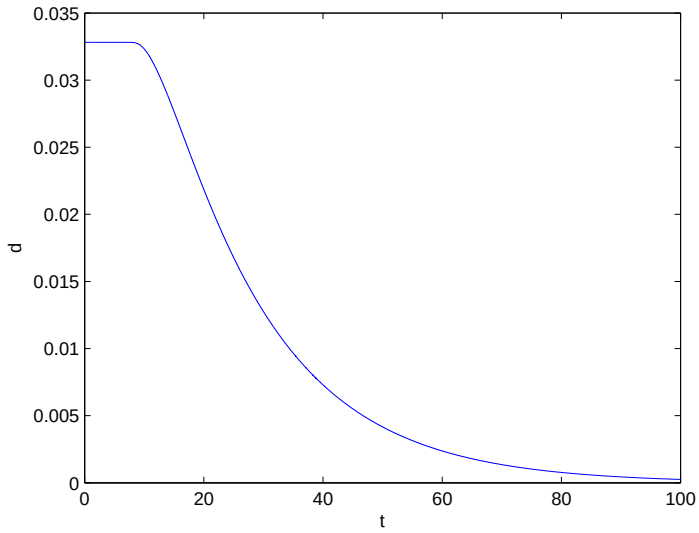

FIGURE 1. Typical density function $d(h,t)$, computed for $g(x,t) = J(x,t)$.

a function of the type

$$g^*(x,t) = g^s(x) + \frac{A(x)}{t_{eff}(x)} e^{\frac{-t}{t_{eff}(x)}}.$$

In this analysis, we use the fact that t_{eff} is the first moment of the exponential distribution (7). Consequently, for any real k, we have

$$P(t \leq kt_{eff}(x)) = 1 - e^{-k}. \tag{10}$$

Using different values of k, an *a priori* flux (or concentration) tracking can be performed as shown for the flux in Table I. The symbol J^s represents the steady-state flux at $x = h$, which can be computed using the Final Value Theorem.

Table 1: Tracking strategy.

t	Flux
t_{eff}	$63.21\%J^s$
$2t_{eff}$	$86.47\%J^s$
$3t_{eff}$	$95.02\%J^s$
$4t_{eff}$	$98.17\%J^s$
$5t_{eff}$	$99.33\%J^s$

Other candidate metrics for estimating the response times have been proposed in the literature. The time lag estimates the onset of the steady-state flux and has been defined [5] as the intercept of the asymptote to the total mass leaving the membrane with the time axis. The cumulative amount is:

$$Q(t) = \int_0^t J(h, s)ds. \tag{11}$$

Several authors ([13], [17]-[16]) have studied, these last years, the time lag for different systems. A statistical interpretation of time lag (t_{lag}) shows that it can be viewed as the mean time of a certain probability density function. However, in many cases, t_{lag} is not an accurate estimation for the onset of equilibrium. In [15], the author shows that, for some problems, the analytical expression of t_{lag} does not reflect the expected dependence on the model parameters.

The first time constant t_1 also provides a measure of the response time and can be obtained from a series solution of the form

$$g(x, t) = g^s(x) + \sum_{n=1}^{\infty} f_n(x)e^{-t/t_n}.$$

To the best of our knowledge, the study of a tracking strategy in the framework of viscoelastic models has not yet been described in the literature. In Section 2, an analytical expression for the effective time constant is computed

for the system represented by Eqs. (1), (2) and (3). As particular cases, effective time constants for Maxwell and Maxwell-Voigt models are analyzed. Their influences on the model parameters (i.e., properties of the polymer and the permeating species) are evaluated. In Section 3, we show how to track the flux and concentration based on a statistical interpretation of t_{eff}. A comparison of our findings with experimental results reported in [9] and [10] confirms the effectiveness of the approach. The tracking strategy is adjusted for overshooting fluxes in Section 4 and pertinent conclusions are drawn in Section 5.

2. Effective time constant

Let us consider the general model represented by Eqs. (1), (2) and (3). We assume that the strain is proportional to the concentration. The integration of equation (2) gives

$$\sigma(x,t) = \int_0^t (\alpha - \gamma\beta) e^{-\beta(t-s)} u(x,s) ds + \gamma u(x,t). \tag{12}$$

The above expression is replaced in equation (1) to yield

$$u_t = D^* u_{xx} + E^* \int_0^t e^{-\beta(t-s)} u_{xx}(x,s) ds, \tag{13}$$

with $D^* = D + D_v\gamma$ and $E^* = D_v(\alpha - \gamma\beta)$. Constants α, β, γ are positive and have well-known physical meanings that will be discussed later. In order to compute the effective time constant we consider in (8) $g(x,t) = J(x,t)$, where the flux J associated with (13),

$$J(x,t) = -D^* u_x - E^* \int_0^t e^{-\beta(t-s)} u_x(x,s) ds, \tag{14}$$

has two components: a Fickian component represented by the first term and a non Fickian one represented by the integral term.

As observed in [6], if the Laplace transform $\overline{J}(x,p)$ of the flux, $\overline{J}(x,p) = \displaystyle\int_0^\infty e^{-pt} J(x,t) dt$, can be represented by

$$\overline{J}(x,p) = \frac{1}{p}(J^s(x) + B(x)p + C(x)p^2), \tag{15}$$

for sufficiently small p, where $J^s(x)$ stands for the steady-state flux, $B(x)$ and $C(x)$ represent functions of x, then the effective time constant defined

in (8) takes the form

$$t_{eff} = -\frac{C(x)}{B(x)}. \tag{16}$$

An expression for $\overline{J}(x,p)$ is computed in this section. As the integral term in (13) is a convolution product, we easily establish that

$$\overline{u}(x,p) = \frac{u_0 \sinh(A(h-x))}{p \sinh(Ah)}, \tag{17}$$

where $\overline{u}$ is the Laplace transform of u and

$$A = \sqrt{\frac{p(p+\beta)}{(D+D_v\gamma)(p+\beta)+D_v(\alpha-\gamma\beta)}}. \tag{18}$$

Using the Final Value Theorem

$$\lim_{t\longrightarrow\infty} u(x,t) = \lim_{p\longrightarrow 0} p\overline{u}(x,p),$$

we deduce that the equilibrium concentration satisfies

$$\lim_{t\longrightarrow\infty} u(x,t) = u_0(1-\frac{x}{h}).$$

From (14) and (17), $\overline{J}$ takes the form

$$\overline{J}(x,p) = -\frac{p\overline{u}_x}{A^2}, \tag{19}$$

that is

$$\overline{J}(x,p) = -\frac{u_0 \cosh(A(h-x))}{A \sinh(Ah)}. \tag{20}$$

Using the Final Value Theorem, we have

$$\lim_{t\longrightarrow\infty} J(x,t) = \lim_{p\longrightarrow 0} p\overline{J}(x,p), \tag{21}$$

and from (20) and (21), the following expression is obtained

$$J^s(x) = \frac{u_0(D\beta + D_v\alpha)}{h\beta}. \tag{22}$$

It was established in [9] that the constant D_v is negative. The authors, using a mesoscopic approach, showed that polymer swelling led to a negative convective flux. As $\frac{u_0 D}{h}$ represents the steady flux of a Fickian diffusion problem, J_F^s, with diffusion coefficient D ([5]), we concluded from (22) that the viscoelastic flux is such that $J^s(x) \leq J_F^s(x)$, where the equality occurs for

$\alpha = 0$. We observe that $J^s(x)$ represents the steady-state flux of a Fickian problem with diffusion coefficient $D + D_v\frac{\alpha}{\beta}$.

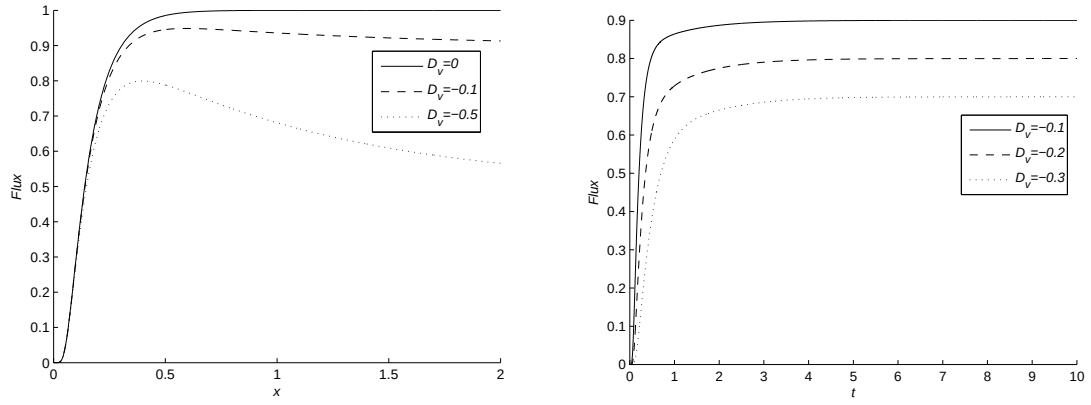

(a) (b)

FIGURE 2. Fluxes with $\alpha = 1$: (a) $\gamma = 0$, $E^* < 0$, (b) $\gamma = 2$, $E^* > 0$.

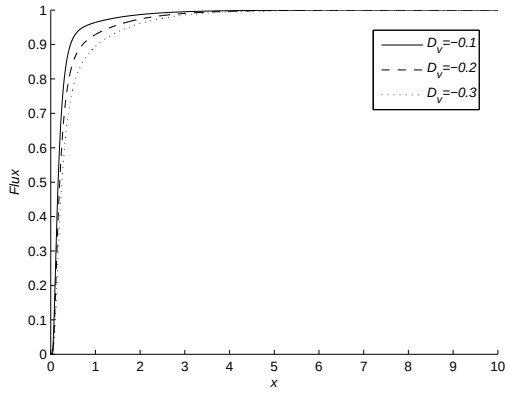

FIGURE 3. Fluxes with $\alpha = 0$ ($\gamma = 1$, $E^* > 0$).

In Figures 2 and 3, the fluxes are shown for different values of D_v, when $\alpha \neq 0$ and $\alpha = 0$, respectively. The flux was computed numerically using the following parameters: $h = 1$, $D = 1$, $u_0 = 1$, $\beta = 1$. Equation (13) was discretized in space using central finite differences and a first-order implicit method was used to integrate in time. In Figure 2-(a), $E^* \leq 0$. The plots exhibited reproduce exactly the flux profiles in Figure 1 of [10]. As $|D_v|$ increases, an overshoot in the flux was observed. In Figure 2-(b), $E^* > 0$.

This behavior is also apparent in the Maxwell-Voigt model as we will establish in what follows. The steady-state value of the flux decreases with $|D_v|$ but, in this case, no overshoot occurs. For $\alpha = 0$ then $J^s(x) = J_F^s(x)$ as illustrated in Figure 3. Profiles of this type, that is fluxes exhibiting a delay but converging to the same steady state (i.e., a pure Fickian equilibrium value), can be found in [9].

If only hyperbolic diffusion is considered, which means that $D = 0$ and $\gamma = 0$, we obtain $J^s(x) = \frac{u_0 D_v \alpha}{h\beta}$, in agreement with the value presented in [17]. In fact, in that paper, the authors study the telegraph equation, $\beta u_t + u_{tt} = D_v \alpha u_{xx}$, with $D_v\alpha$ depending on u. Under certain conditions, with $D_v\alpha$ constant, this equation is equivalent to (13).

Let us now compute the effective time constant. We begin by considering in (8) $g(x,t) = J(x,t)$. For p small we have, from (20),

$$\overline{J}(x,p) = u_0 \frac{1 + \frac{A^2(h-x)^2}{2} + \frac{A^4(h-x)^4}{4!} + ...}{A^2 h + \frac{A^3 h^3}{3!} + \frac{A^6 h^5}{5!} + ...}. \tag{23}$$

Approximating A^2 by

$$A^2 = p\frac{\beta}{k} + \frac{p^2}{k^2}E^* + \mathcal{O}(p^3), \tag{24}$$

with $k = D^*\beta + E^*$, we can give (23), after some tedious but straightforward computations, the form (15), and finally using (16) we establish that for $x = h$

$$t_{eff}^f = \frac{1}{D^*\beta + E^*}\left(\frac{E^*}{\beta} + \frac{\beta h^2}{3!} + \frac{D^*E^*h - 2\beta E^*\frac{h^3}{3!} - \beta^3\frac{h^5}{5!}}{E^*h + \beta^2\frac{h^3}{3!}}\right). \tag{25}$$

The effective time constant can be computed for any x. However, within release technology, the focus is placed on its value at $x = h$. Following the procedure outlined above, the effective time constant (6) can be defined using the concentration $g(x,t) = u(x,t)$, obtaining

$$t_{eff}^c(x) = \frac{1}{\beta(D^*\beta + E^*)}(-E^* + \frac{\beta^2 h^2}{60}(7 - 3(1 - \frac{x}{h})^2)). \tag{26}$$

For a pure diffusion problem ($D_v = 0$) we obtain, from (25) and (26), the expression

$$t_{eff}^f = t_{eff}^c = \frac{7h^2}{60D},$$

presented in [6]. A rationale for the calculation of t^c_{eff} in terms of any x is offered in Section 3 along with a comparison between the values of effective time given by (25) and (26). In what follows, we study particular cases of problem (1)-(2)-(3) which correspond to well-known models in the viscoelastic literature.

The classical approach to derive viscoelastic constitutive models is through the use of mechanical analogs that are simple mechanical models for fluid and solid combined to produce viscoelastic effects. The simplest mechanical analog for a linear elastic material is a spring; the mechanical analog for a Newtonian fluid is a dashpot. Combining these analogs in several ways we can obtain the class of models referred in the introduction, among others. To shorten the presentation, only Maxwell-Voigt models are described. The Maxwell model is studied as a particular case of the latter class.

(1) ***Maxwell-Voigt model and Maxwell model***

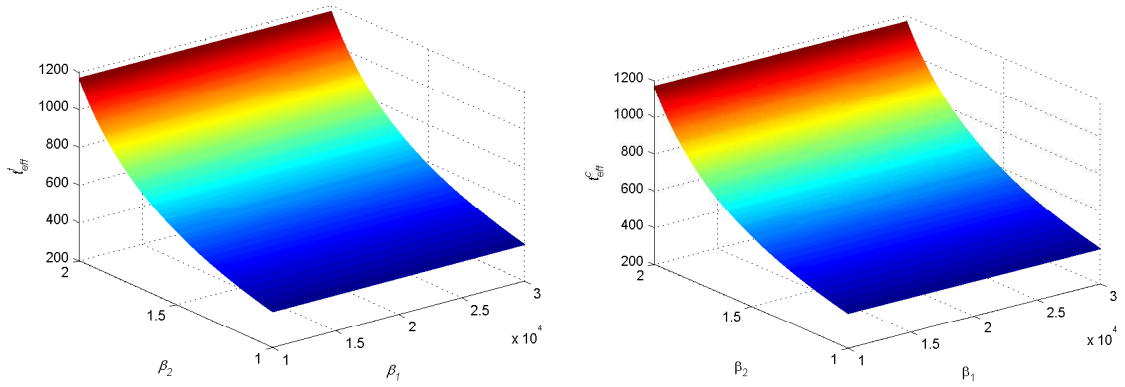

FIGURE 4. Behavior of t^f_{eff} (a) and t^c_{eff} (b), for Maxwell-Voigt model.

Maxwell-Voigt model [1] results from considering the local behavior of the polymer modeled using a damper in parallel with a spring and the whole structure in series with a second spring. Representing by $\beta_1+\beta_2$ the Young modulus of the springs and by η the viscosity of the damper we can establish that the relation between stress and strain is defined by

$$\frac{\eta}{\beta_1+\beta_2}\sigma_t+\sigma=\frac{\beta_1\beta_2}{\beta_1+\beta_2}u+\frac{\beta_2\eta}{\beta_1+\beta_2}u_t. \tag{27}$$

Equation (27) is a particular case of (2) obtained when $\beta = \frac{\beta_1+\beta_2}{\eta}$, $\alpha = \frac{\beta_1\beta_2}{\eta}$ and $\gamma = \beta_2$.

Considering their physical meaning it is obvious that β_1, β_2, η and D are positive constants. As stated in [9] and [10], there is physical evidence that $D_v < 0$. Considering $D_v < 0$ and observing that for Maxwell-Voigt model $\alpha - \gamma\beta = -\frac{\beta_2^2}{\eta} < 0$ we have $E^* > 0$. Analyzing equation (13) we can interpret it is a modified Fickian diffusion equation where the diffusion coefficient D is replaced by $D^* = D + D_v\gamma < D$ and the memory term

$$\frac{-D_v\beta_2^2}{\eta}\int_0^t e^{-\frac{\beta_1+\beta_2}{\eta}(t-s)}u_{xx}(x,s)ds$$

is considered to balance the decrease in the Fickian diffusion.

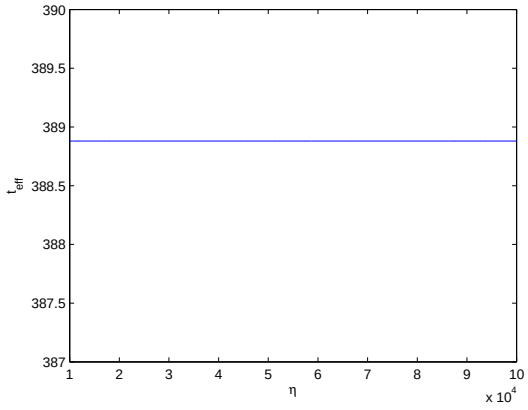

FIGURE 5. Behavior of t_{eff}^f for Maxwell-Voigt model.

In Figure 4, t_{eff}^f and t_{eff}^c are plotted as a function of β_1 and β_2 , for a fixed viscosity $\eta = 10^5 Pa.s$. To obtain Figures 4 and 5, the following parameters were used: $D_v = -2 \times 10^{-10} m^3 s/moles$, $D = 5 \times 10^{-10} m^2/s$, $h = 1 \times 10^{-3} m$. As expected, the two plots present the same behavior. In Figure 5, the behavior of t_{eff}^f in function of η and for a fixed $\beta_1 + \beta_2 = 0.3 \times 10^5 Pa$ is displayed. We note that t_{eff}^f is an increasing function of the Young modulus, for a fixed viscosity. The effective time constant is not sensitive to the variation of the viscosity in the range investigated. Several experimental studies in the literature report the increasing behavior of time release with the

Young modulus and viscosity ([2],[3]). The domain of β_2 is defined by the restriction $D + D_v\beta_2 > 0$.

A particular case of the Maxwell-Voigt model is the Maxwell model, which is obtained by connecting in series a purely viscous damper and a purely elastic spring and assuming that strain is proportional to the concentration of the permeating species. The model is described by ([4], [7], [1])

$$\eta\sigma_t + \beta_2\sigma = \beta_2\eta u_t,$$

where β_2 represents the elastic modulus and η the material coefficient of viscosity. The last equation is obtained by letting $\beta_1 \longrightarrow 0$ in (27).

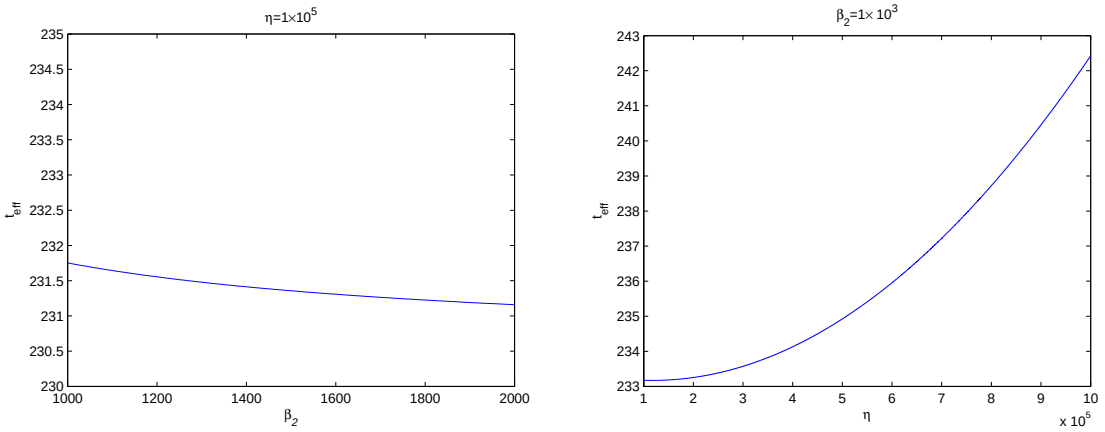

(a) (b)

FIGURE 6. Behavior of t_{eff} for Maxwell model, when t_{eff} is a function of β_2 (a) or η (b).

We show in Figure 6 the behavior of the effective time constant with varying β_2 and η for the Maxwell model when $D = 5\times10^{-10}m^2/s$, $D_v = -2 \times 10^{-14}m^3s/moles$ and $h = 10^{-3}m$. The parameter $\tau = \frac{\eta}{\beta_2}$ represents the relaxation time constant of the polymer. The relative variation of t_{eff} with η, for the range of values in the figure, is much more significant than its variation with β_2, which agrees with the fact that Maxwell is a better representation of a viscoelastic fluid. Such a material relaxes completely to zero stress, when responding to an instantaneous strain, and undergoes a continuously increasing strain under a step stress [1]. We remark that the behavior of effective time with β_2 is not physical even if t_{eff} decreases very slightly with β_2.

(2) ***Effective time for the phenomenological model in*** [10]
In [10] the authors consider the viscoelastic behavior of the polymer described by equation

$$\sigma_t + \frac{1}{\beta_1}\sigma = \frac{\eta}{\beta_1}u + \frac{\eta\beta_2}{\beta_1}u_t$$

where β_1 represents the relaxation time, β_2 the retardation time and η the viscosity. The work is illustrated with a set of simulations and numerical experiments, that we will comment in Section 3 and 4, characterized by $E^* < 0$. In this case, the flux profiles present overshoots and effective time must be computed with concentration, using (26). In Figure 7 we exhibit a plot of t^c_{eff} to illustrate its behavior with viscosity and relaxation time, where we used the parameters $h = 10^{-3}$, $D = 10^{-10}$, $D_v = -10^{-15}$, $\beta_2 = 0$. We observe that t_{eff} is an increasing function of the retardation time β_1 for constant viscosity, and an increasing function of the viscosity η for constant retardation time β_2.

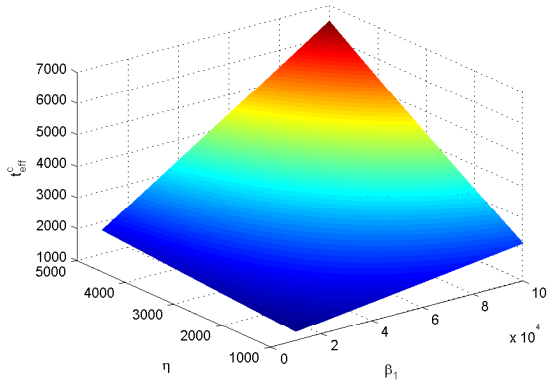

FIGURE 7. Behavior of t_{eff}.

3. Flux and concentration tracking

The influence of the mechanic properties of the polymeric matrix on the steady flux and the effective time was analyzed in Section 2. Dimensional equations were considered in order to understand the effects of individual physical parameters on the process dynamics. In this section, we present a flux tracking strategy that consists of a set of *a priori* estimations of fluxes

and the times it takes to reach these points. Interpreting t as a statistic variable with the exponential density function (7), $g(x,t) = u(x,t)$ or $g(x,t) = J(x,t)$, a concentration or a flux tracking strategy can be devised. The methodology is illustrated using two models. First, we consider the Maxwell-Voigt model, for which $E^* > 0$ and presenting no overshoots in the flux and the concentration profiles. As t^c_{eff} and t^f_{eff} represent the first moment of the density distribution function (7), then for any real k we have

$$P(t \leq kt_{eff}) = 1 - e^{-k},$$

where t_{eff} represents both t^c_{eff} and t^f_{eff}. As reported in (22), the steady-sate flux or concentration can be estimated for any k, giving

$$\widetilde{u}(x, kt^c_{eff}) = (1 - e^{-k})u_0(1 - \frac{x}{h}), \tag{28}$$

$$\widetilde{J}(x, kt^f_{eff}) = (1 - e^{-k})\frac{u_0(D\beta + D_v\alpha)}{h\beta}. \tag{29}$$

The boundary condition at $x = h$ is $u(h,t) = 0$ leading to $\overline{u}(h,t) = 0$, and equation (28) gives no valuable information. Given that the permeant is immediately removed (i.e., sink condition at $x = h$), we consider that the steady-state drug concentration at $x = h$ is $u(h - \Delta x, kt^c_{eff}) = u_0\frac{\Delta x}{h}$, where Δx is a stepsize relatively small.

To compare our predictions with the experimental results in [10] we adimensionalize equation (1)(2)(3), obtaining

$$\begin{cases} u^*_t = u^*_{xx} + \gamma_1\sigma^*_{xx}\,,\ x^* \in (0,1), t^* > 0 \\ \\ \gamma_2\sigma^*_t + \sigma^* = u^* + \gamma_3 u^*_t\,,\ x^* \in (0,1), t^* > 0 \\ \\ u^*(x^*,0) = 0, \sigma^*(x^*,0) = 0,\ x^* \in (0,1) \\ \\ u^*(0,t) = 1,\ u^*(1,t^*) = 0,\ t^* > 0 \end{cases},$$

where $u^* = \dfrac{u}{u_0}$, $x^* = \dfrac{x}{h}$, $\sigma^* = \dfrac{\sigma\beta}{u_0\alpha}$, $t^* = \dfrac{t}{h^2/D}$, $\gamma_1 = \dfrac{D_v\alpha}{D\beta}$, $\gamma_2 = \dfrac{1}{\beta(h^2/D)}$, $\gamma_3 = \dfrac{\gamma}{\alpha(h^2/D)}$. In what follows the superscrit $*$ will be omitted. We illustrate flux tracking for problem (1), (2), (3) and (4) where in the mechanical model (2) the parameters are selected in order to satisfy the Maxwell-Voigt model and the phenomenological method presented in [10].

We begin by presenting flux and concentration tracking for Maxwell-Voigt. In this case, $E^* > 0$ and there is no overshoots in the flux and in the concentration profiles. The estimated and numerical fluxes are presented in Table 2.

Table 2: Flux tracking-with
$D = 1, h = 1, \gamma_1 = -0.1,\ \gamma_2 = 0.5,\ \gamma_3 = 0.6,\ u_0 = 1.$

Effective time	Estimated Flux	Numerical flux	Relative Error
$t_{eff} = 0.151$	$63.21\% J^s = 0.56889$	0.4159621	2.68818×10^{-1}
$2t_{eff} = 0.301$	$86.47\% J^s = 0.77823$	0.758114	2.58484×10^{-2}
$3t_{eff} = 0.452$	$95.02\% J^s = 0.85518$	0.856987	2.1130×10^{-3}
$4t_{eff} = 0.602$	$98.17\% J^s = 0.88353$	0.885031	1.69887×10^{-3}
$5t_{eff} = 0.753$	$99.33\% J^s = 0.89397$	0.893596	4.18359×10^{-4}

A concentration tracking can also be performed as shown in Table 3.

Table 3: Concentration tracking- with
$D = 1, h = 1, \gamma_1 = -0.1,\ \gamma_2 = 0.5,\ \gamma_3 = 0.6,\ u_0 = 1.$

Effective time	Est. Concent.	Num. Concent.	Relative Error
$t_{eff} = 0.119$	$63.21\% u^s = 6.321 \times 10^{-3}$	3.20753×10^{-3}	4.926×10^{-1}
$2t_{eff} = 0.237$	$86.47\% u^s = 8.647 \times 10^{-3}$	7.46871×10^{-3}	1.363×10^{-1}
$3t_{eff} = 0.356$	$95.02\% u^s = 9.502 \times 10^{-3}$	9.12848×10^{-3}	3.93×10^{-2}
$4t_{eff} = 0.474$	$98.17\% u^s = 9.817 \times 10^{-3}$	9.71604×10^{-3}	1.03×10^{-2}
$5t_{eff} = 0.593$	$99.33\% u^s = 9.933 \times 10^{-3}$	9.92332×10^{-3}	9.745×10^{-4}

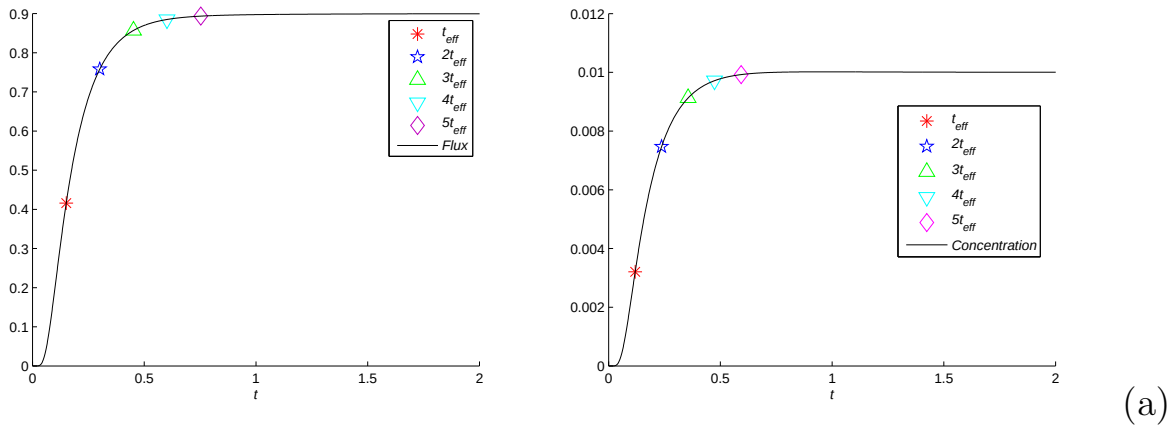

(a)

(b)

FIGURE 8. Flux Tracking with data of Table 2 (a) and Concentration Tracking with data of Table 3 (b).

The methodology is applied now to the phenomenological model discussed in [10]. Experiments and simulations were conducted for $E^* < 0$. Section 2

shows that such cases result in an overshoot relative to the desired steady-state value. Consequently, equation (6) can not be used with $g(x,t) = J(x,t)$. To calculate the effective time, $g(x,t) = u(x,t)$ should be then used. In Section 4, an alternative definition for estimating t^f_{eff} in case of overshoots is presented [6].

Table 4: Concentration tracking-
$u_0 = 1$, $D = 1$, $h = 1$, $\gamma_2 = 1$, $\gamma_3 = 0, \gamma_1 = -0.1$.

Effective time	Est. Concent.	Num. Concent.	Relative Error
$t_{eff} = 0.241$	$63.21\%u^s = 6.32098 \times 10^{-3}$	8.01426×10^{-3}	0.26788
$2t_{eff} = 2.467$	$86.47\%u^s = 8.64698 \times 10^{-3}$	9.70035×10^{-3}	0.1218
$3t_{eff} = 0.7222$	$95.02\%u^s = 9.50197 \times 10^{-3}$	9.87731×10^{-3}	3.950×10^{-2}
$4t_{eff} = 0.963$	$98.17\%u^s = 9.81697 \times 10^{-3}$	9.91186×10^{-3}	9.666×10^{-3}
$5t_{eff} = 1.203$	$99.33\%u^s = 9.93297 \times 10^{-3}$	9.92978×10^{-3}	3.210×10^{-4}

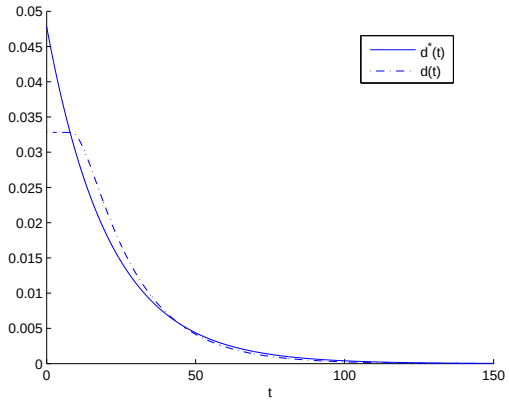

FIGURE 9. An exponential density function $d^*(t)$ (9) vs the plot of $d(t)$ (7).

We observe that for $t = t^f_{eff}$ or $t = t^c_{eff}$ the results are not accurate. In fact, the estimated flux is computed assuming the ansatz that the distribution density function is of form $d^*(t) = \dfrac{1}{t_{eff}} e^{-t/t_{eff}}$. The plot of d computed with the flux and the graph of d^* shows that, at small time, d does not follow an exponential trend (Figure 9).

Remark- We already noted that when $\alpha = 0$, that is when the Maxwell model is considered, fluxes converge to a steady Fickian flux J^s_F. In Figure 10, the flux is plotted for different values of $\tau = \frac{1}{\beta}$, where τ represents the relaxation time. At small times, there is a delay which increases with relaxation time. However, we observe a curious phenomena for large times:

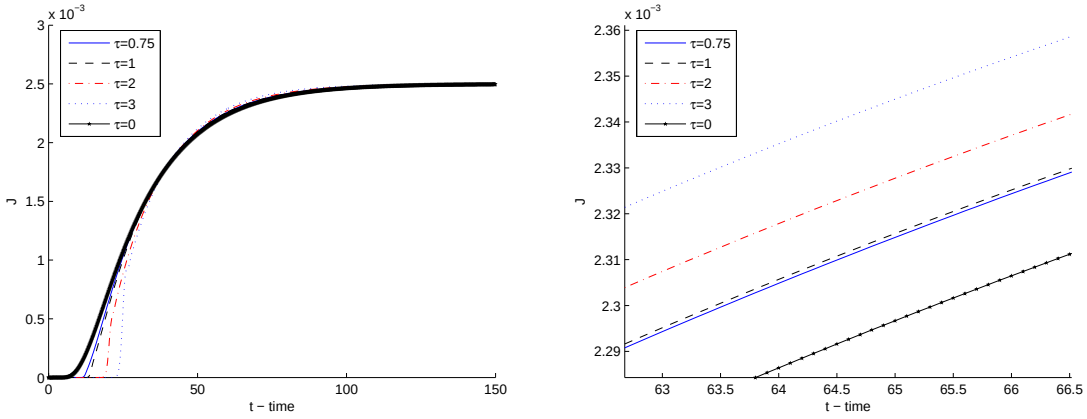

FIGURE 10. Behavior of flux for Maxwell model, for different value of τ.

the larger is τ, the larger is that flux. This kind of inversion can be observed in Figure 10 and also in Table 5, where effective time, t^f_{eff} is a decreasing function of relaxation time. Profiles of this type, where fluxes exhibit delays before converging to the same Fickian steady state can be also found in [9].

Table 5: Effective time.

τ	t^f_{eff}
0	93.33
0.75	92.13
1	91.75
2	90.37
3	89.17

4. Response times for overshooting fluxes

When $E^* < 0$ the fluxes profiles present overshoots with amplitudes that increase with $|D_v|$. In this case, we outlined in Section 3 a tracking strategy based on t^c_{eff}, that is an effective time defined from (6) with $g(x,t) = u(x,t)$. Another alternative is suggested in [6] where, for the cases of overshoots profiles, the effective time is redefined as

$$t^{(2)}_{eff}(x) = 2\frac{\int_0^\infty t(g^s(x) - g(x,t))^2 dt}{\int_0^\infty (g^s(x) - g(x,t))^2 dt},$$

which can be interpreted as the first moment of

$$t_{eff}^{(2)}(x) = 2\frac{(g^s(x) - g(x,t))^2}{\int_0^\infty (g^s(x) - g(x,t)^2 dt}.$$

As an analytical expression for $t_{eff}^{(2)}(x)$ is not yet available, we have computed it at $x = h$ numerically using a time large enough to approximate the improper integrals. We present in Figure 11 the plots of the fluxes for the parameter values listed in Table 3. In Table 6 we compare t_{eff}^{c} with $t_{eff}^{(2)}$. We note that for every plot the first star signals t_{eff} and the second are represents $4t_{eff}$.

Table 6: Effective time.

	t_{eff}^{c}	$t_{eff}^{(2)}$
$\gamma_3 = -0.1$	0.241	0.164
$\gamma_3 = -0.3$	0.595	0.614
$\gamma_3 = -0.5$	1.233	1.229

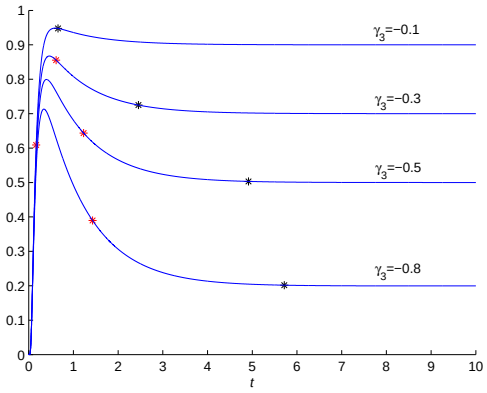

FIGURE 11. Behavior of flux for $E^* < 0$

5. Conclusions

A methodology was proposed to compute, based on the time constant, *a priori* estimates of the flux and concentration profiles of molecules diffusing through polymeric membranes. In the systems studied, mass transport was controlled by diffusion and stress. The developed procedure allows researchers to directly link physicochemical properties of the permeant/membrane system to the transient process behavior. The Maxwell-Voigt

and Maxwell models were selected to demonstrate the suitability of the strategy to predict viscoelastic diffusion. Expressions for the concentrations and flux along the length of a thin membrane were first derived in the Laplace domain. An effective time constant parameter was derived in this context. The effective time constant increased with the Young Modulus and did not change with the range of viscosities studied (i.e., 1 to 10^5 Pa.s) in the case of the Maxwell-Voigt model. When simulations were conducted using the Maxwell model, results show that this dynamic measure increased with the polymer relaxation time for a constant Young Modulus. Considering transport across swelling membranes, the effective time constant is an increasing function of the retardation time and the viscosity. In the absence of overshoot, the accuracy of the predictions of the flux and concentration increased as the process approached steady state. At four and two time constants, the errors in the delivery rate were 0.20 and 2.65 percent, respectively. As the retardation time increased, more time was required to develop steady-state concentrations and flux for processes exhibiting overshoots.

6. Appendix

Let us consider

$$\begin{cases} u_t = Du_{xx} + D_v\sigma_{xx},\ x \in (0,h), t > 0 \\ \sigma_t + \beta\sigma = \alpha u + \gamma u_t\ ,\ x \in (0,h), t > 0 \\ u(0,t) = u_0, t > 0 \\ J(h,t) = -\mu u(h,t), t > 0 \\ u(x,0) = \sigma(x,0) = 0, x \in (0,h) \end{cases} . \tag{30}$$

Processing as before we can establish that

$$\overline{J}(h,t) = \frac{u_0}{A}\frac{p\sinh(A(h-c)) + \mu\cosh(A(h-c))}{p\cosh(Ah) + \mu\sinh(Ah)} \tag{31}$$

where A is defined in (18). If in (31) we consider $x = h$ we finally have

$$\overline{J}(h,t) = \frac{\mu u_0}{p\cosh(Ah) + \mu A\sinh(Ah)}. \tag{32}$$

To compute effective time we give to (32) the form (15) and using then (16), we establish, after some tedious but straight forward computations, that

$$t_{eff} = \frac{\mu h E^* + \frac{\beta k h^2}{2!} + \frac{\mu\beta^3 h^3}{3!}}{k(k+\mu\beta h)} - \frac{1}{k}\frac{-\mu D^* h E^* + E^* k\frac{h}{2!} + \frac{2\mu\beta E^* h^3}{3!} + \frac{\beta^2 k h^4}{4!} + \frac{\beta^3\mu h^5}{5!}}{\mu h E^* + \frac{\beta k h^2}{2!} + \frac{\beta^2\mu h^3}{3!}}.$$

We note that taking limits when $\mu \longrightarrow \infty$ we obtain equation (25).

References

[1] Hal F. Brinson and C. Brinson, Polymer Engineering Science and Viscoelasticity: An introduction, *Springer*, NY, 2008.

[2] L.W.S. Cheong, P.W.S. Heng, L.F. Wong, Relationship between polymer viscosity and drug release from a matrix system, *Pharm. Res*, 9-11, 1992.

[3] S. Cypes, W.M. Saltzman, E.P. Gianneli, Organosilicate polymer drug delivery systems: controlled release and enhanced machanical properties *J. Cont. Release*, 90, 163-169, 2003.

[4] D.S. Cohen, B. White, Sharp fronts due to diffusion and viscoelastic relaxation in polymers *SIAM J. Appl Math.*, 51, 472-483, 1991.

[5] J. Crank. The mathematics of diffusion *Oxford University Press*, 1976.

[6] R. Collins, The choise of an effective time constant for diffusive processes in finite systems, *J. Phys. D: Appl. Phyps.*, 13, 1935-1947, 1980.

[7] R.W. Cox, D.S. Cohen, A mathematical model for stress-driven diffusion in polymers, *J. Pol. Sci. B. Pol. Phys.*, 27, 589-602, 2003.

[8] E. Favre, N. Morliere, D. Roizard, Experimental evidence and implications of an imperfect upstream pressure step for the time-lag technique, *J. Memb. Sci.*, 207, 59-72, 2002.

[9] Q. Liu, D.De Kee, Modeling diffusion through polymeric membranes, *Rheol. Acta.*, 44, 287-294, 2005.

[10] Q. Liu, X. Wang, D. De Kee, Mass transport through swelling membranes, *Int. J. Eng. Sci.*, 43, 1464-1470, 2005.

[11] R.A. Siegel, R. Langer, Mechanistic studies of macromolecular drug release from macroporous polymers, II Models for the slow kinetics of drug release, *J. Cont. Release*, 14, 153-167, 1990.

[12] L. Simon, Analysis of heat-aided membrane controlled drug released from a process control prespective, *Int. J. Heat Mass Transfer*, 50, 2425-2433, 2007.

[13] L. Simon, Timely drug delivery from controlled-release devices: Dynamic analysis and novel design concepts, *Math. Biosci.*, 217, 151-158, 2009.

[14] R.A. Siegel, E.L. Cussler, Reactive barrier membranes: some theoretical observations regarding the time lag and breakthrough curves, *J. Memb. Sci.*, 229, 33-41, 2004.

[15] R.A. Siegel, Characterization of relaxation to steady state in membranes with binding and reaction, *J. Memb. Sci.*, 251, 91-99, 2004.

[16] A. Strzelewicz, Z.J. Grzywna, Studies on the air membrane separation in the presence of a magnetic field, *J. Memb. Sci.*, 294, 60-67, 2007.

[17] A. Strzelewicz, Z. J. Grzywna, On the permeation time lag for different transport equations by Frisch method *J. Memb. Sci.*, 322, 460-465, 2008.

[18] S. Xiao, C. Moresoll, J. Bovenkamp,D. De Kee, Sorption and permeation of organic environmental contaminants through PVC geomembranes, *J. Appl. Polym. Sci.*, 63, 1189-1197, 1997.

CMUC,Department of Mathematics, University of Coimbra, Apartado 3008, 3001-454 Coimbra, Portugal

E-mail address: ferreira@mat.uc.pt
URL: http://www.mat.uc.pt/~ferreira

P. de Oliveira
CMUC,Department of Mathematics, University of Coimbra, Apartado 3008, 3001-454 Coimbra, Portugal

E-mail address: poliveirt@mat.uc.pt

P. M. da Silva
Department of Physics and Mathematics, ISEC, Rua Pedro Nunes, Quinta da Nora, 3030-199 Coimbra, Portugal

E-mail address: pascals@isec.pt

L. Simon
Department of Chemical, Biological and Pharmaceutical Engineering, New Jersey Institute of Technology Otto H. York, Newark, New Jersey, USA

E-mail address: laurent.simon@njit.edu